AD-A104 152 COAST GUARD RESEARCH AND DEVELOPMENT CENTER GROTON CT F/G 8/12
BRASH ICE BEHAVIOR.(U)
MAY 81 P GREISMAN
UNCLASSIFIED CGR/DC-9/81 USCG-30-81 NL

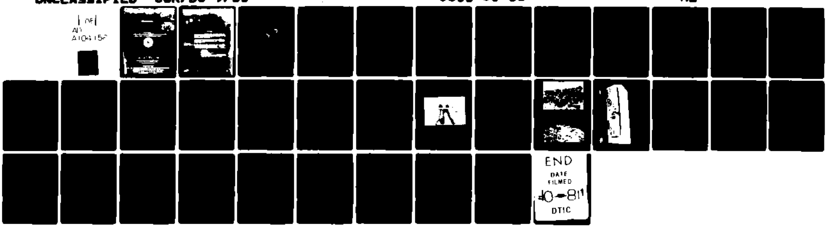

Technical Report Documentation Page

1. Report No.: CG-D-30-81

2. Government Accession No.: AD-A104 152

3. Recipient's Catalog No.:

4. Title and Subtitle: BRASH ICE BEHAVIOR

5. Report Date: MAY 1981

6. Performing Organization Code:

7. Author(s): PAUL GREISMAN

8. Performing Organization Report No.: CGR/DC-9/81

9. Performing Organization Name and Address:
United States Coast Guard
Research and Development Center
Avery Point
Groton, Connecticut 06340

10. Work Unit No. (TRAIS)

11. Contract or Grant No.

12. Sponsoring Agency Name and Address:
Department of Transportation
United States Coast Guard
Office of Research and Development
Washington, DC 20593

13. Type of Report and Period Covered: FINAL REPORT

14. Sponsoring Agency Code

15. Supplementary Notes

16. Abstract

The behavior of brash ice, its formation and recommended vessel operating procedures are presented.

Brash ice behaves as a Mohr-Coulomb solid below a critical strain rate or ship speed. Above this speed, fluidization of the medium occurs and the resistance appears to be that of a viscous, laminar fluid.

The optimum operating speed for a vessel in brash is at the viscous threshold, found here to be $0.12\sqrt{gL}$ where g (32.2 fS^{-2}) is the acceleration of gravity and L is the length of the vessel.

Repeated passages through brash-filled channels to keep them unconsolidated are generally unadvisable due to the attendant enhancement of the accretion rates.

The laboratory and field experiments employed in this study are presented. Laboratory tests in brash ice appear to yield very useful results that are good predictors of full-scale resistance.

17. Key Words: brash ice, rheology, ice-clogged channel

18. Distribution Statement: This document is available to the U.S. public through the National Technical Information Service, Springfield, Virginia 22161

19. Security Classif. (of this report)	20. Security Classif. (of this page)	21. No. of Pages	22. Price
UNCLASSIFIED	UNCLASSIFIED		

METRIC CONVERSION FACTORS

Approximate Conversions to Metric Measures

Symbol	When You Know	Multiply by	To Find	Symbol
		LENGTH		
in	inches	*2.5	centimeters	cm
ft	feet	30	centimeters	cm
yd	yards	0.9	meters	m
mi	miles	1.6	kilometers	km
		AREA		
in^2	square inches	6.5	square centimeters	cm^2
ft^2	square feet	0.09	square meters	m^2
yd^2	square yards	0.8	square meters	m^2
mi^2	square miles	2.6	square kilometers	km^2
	acres	0.4	hectares	ha
		MASS (weight)		
oz	ounces	28	grams	g
lb	pounds	0.45	kilograms	kg
	short tons (2000 lb)	0.9	tonnes	t
		VOLUME		
tsp	teaspoons	5	milliliters	ml
Tbsp	tablespoons	15	milliliters	ml
fl oz	fluid ounces	30	milliliters	ml
c	cups	0.24	liters	l
pt	pints	0.47	liters	l
qt	quarts	0.95	liters	l
gal	gallons	3.8	liters	l
ft^3	cubic feet	0.03	cubic meters	m^3
yd^3	cubic yards	0.76	cubic meters	m^3
		TEMPERATURE (exact)		
°F	Fahrenheit temperature	5/9 (after subtracting 32)	Celsius temperature	°C

*1 in = 2.54 (exactly). For other exact conversions and more detailed tables, see NBS Misc. Publ. 286, Units of Weights and Measures, Price $2.25, SD Catalog No. C13.10:286.

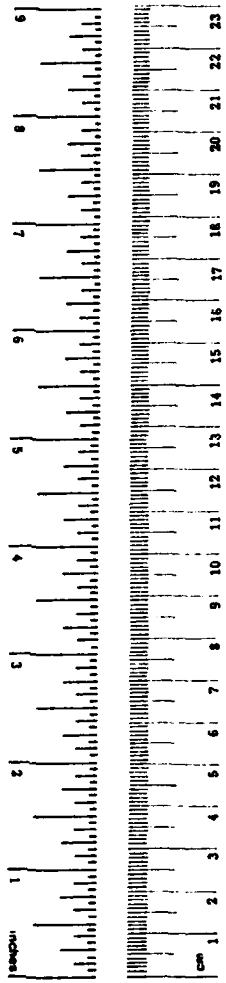

Approximate Conversions from Metric Measures

Symbol	When You Know	Multiply by	To Find	Symbol
		LENGTH		
mm	millimeters	0.04	inches	in
cm	centimeters	0.4	inches	in
m	meters	3.3	feet	ft
m	meters	1.1	yards	yd
km	kilometers	0.6	miles	mi
		AREA		
cm^2	square centimeters	0.16	square inches	in^2
m^2	square meters	1.2	square yards	yd^2
km^2	square kilometers	0.4	square miles	mi^2
ha	hectares (10,000 m^2)	2.5	acres	
		MASS (weight)		
g	grams	0.035	ounces	oz
kg	kilograms	2.2	pounds	lb
t	tonnes (1000 kg)	1.1	short tons	
		VOLUME		
ml	milliliters	0.03	fluid ounces	fl oz
l	liters	2.1	pints	pt
l	liters	1.06	quarts	qt
l	liters	0.26	gallons	gal
m^3	cubic meters	35	cubic feet	ft^3
m^3	cubic meters	1.3	cubic yards	yd^3
		TEMPERATURE (exact)		
°C	Celsius temperature	9/5 (then add 32)	Fahrenheit temperature	°F

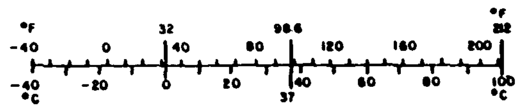

ACKNOWLEDGEMENT

Dr. George Vance (formerly of the U.S. Coast Guard, formerly of the U.S. Army CRREL and currently of Mobil Research and Development Corp.) aided me immeasurably in the laboratory work at CRREL. He was both an inspiration and an invaluable expeditor at CRREL in January 1980. LCDR Pete Tebeau cheerfully worked with me both in the laboratory and in the field under often difficult circumstances.

TABLE OF CONTENTS

LIST OF ILLUSTRATIONS

LIST OF TABLES

1.0 INTRODUCTION

Repeated passages of vessels through shipping channels in ice-covered water are responsible for the accumulation of brash ice. After the initial breaking of the level ice the individual ice pieces are modified in size, shape and concentration (as described below) with the eventual result of a channel filled with chunks of ice. The thickness of the brash is usually considerably greater than the thickness of adjoining level ice and in heavily travelled channels such as the Detroit River, the brash can fill the entire channel to the bottom.

The brash ice does not behave in a mechanically similar manner to level ice. It can impede vessel motion and trap low powered vessels. If undisturbed with cold air temperature for periods of a day or so, freezing bonds form between the individual pieces and the channel must be "rebroken." However, even in the absence of refreezing, the brash can be an impenetrable barrier to shipping.

The Coast Guard is responsible for navigation in inland waters and the Polar regions. In these regions, brash ice is encountered after the initial ice breaking is performed. A description of the very unique brash ice substance and a theory of its behavior is presented here. Hopefully, this information will be of use in ice breaking operations and the design of clogged channel clearing devices.

2.0 DESCRIPTION OF BRASH ICE

The first problem encountered in this study involved nomenclature. The ice terminology vocabulary draws from several languages and may be confusing to all but the experts. The World Meteorological Organization Sea-Ice Nomenclature is extremely useful in alleviating much of this confusion. According to this nomenclature, the blocks of ice which are found in shipping channels can be classified as "Brash Ice." This term applies to discrete pieces of ice less than 2m in size. Brash ice does not include rafted features, or pressure ridges; it refers to floating discrete pieces of ice.

The brash ice which is formed in shipping channels can be further characterized. After many ship transits, the initial wreckage of the level ice sheet is "processed" by the motion of the hull through the water-rubble mixture. The "processed" brash ice gradually assumes an equilibrium distribution of sizes and the shape of the individual pieces approaches spheroidal. This "equilibrium" shipping channel brash ice might better be termed "cannonball ice" - certainly a more descriptive term. It would be useful to determine a size versus frequency distribution of the brash components but this has not been, to date, possible. Individual pieces up to 3 m in size have been noted by Sandkvist (1980) and there is certainly some frazil (fine spicules of ice less than 1 or 2 mm) present in the brash. An estimate of the median size of the distribution might be about 1 m or smaller.

The essence of the brash ice medium in shipping channels is that the pieces be more than one layer thick. This is a universally observed characteristic and is extremely important in understanding the nature of the medium. In order for the pieces to be stacked 2 or more deep a lateral restraining force is essential to balance the pseudo-hydrostatic and gravity forces which tend to spread the pieces to a uniform 1 layer thickness. Brash ice in channels can only be understood if the lateral restraining force is kept in mind. In certain natural systems, brash ice can occur if the wind stress is such as to induce a closing of the level ice sheet along the channel axis. More common, however, is for the banks of the channel to supply the reaction force necessary. In fact, the distribution of brash ice thickness across a channel shows very pronounced thickening at the edge of the level ice. These submerged "walls" of brash ice must form before the brash accumulation in the channel can progress very far. Figure 1 is a schematic cross section of a shipping channel filled with brash. The "walls" near the channel side can be 2 or 3 times thicker than the brash in the center of the channel. h is the thickness of the brash ice and Φ the angle of repose.

The brash ice which is found in shipping channels differs in appearance and behavior from naturally occurring fragmented ice types which are often, confusingly, termed brash. For example, relatively thin ice may be fractured and then rafted over adjacent floes. The rafting or the collision of a floe with the shore can produce rubble. This sort of ice can be distinguished from the brash found in channels by the angularity of the individual pieces. This naturally occurring brash is not subjected to repeated disturbance due to vessel traffic and therefore retains its sharp edges and corners and somewhat flattened, plate-like shape.

Another form of ice with which the "cannonball" brash ice should not be confused is slush ice or mush ice. Slush is defined as accumulation of snow in water, but either of these terms refers to small ice crystals (less than 1 cm or so maximum size) completely saturated with water. This ice type is not one which usually forms in channels and hinders navigation.

3.0 FORMATION OF BRASH ICE

In order to better understand the brash ice medium, we undertook an inquiry into its genesis. The most useful component of the inquiry was not the literature but rather the laboratory and field experiments which are described in detail in Section 4.2. Our perception of the formation process follows.

The initial condition for the formation of brash ice is a level parent ice sheet. The ice may be fresh or saline. Once the first vessel transit is accomplished, the salt content (or strength) of the ice is no longer important. The first vessel transit through the level ice breaks the ice into tabular pieces of thickness equal to the thickness of the parent ice sheet and horizontal dimension roughly comparable with the characteristic length scale of the ice medium. This scale is determined by the thickness, Young's Modulus, tensile strength, and Poisson's ratio of the ice.

Depending upon the hull form, differing amounts of ice will remain in the channel. From experiments performed in an ice-covered towing tank at the U.S. Army Cold Region Research and Engineering Lab, we found that a scale model of a 140-foot icebreaker hull, being efficiently designed, allowed most of the broken pieces to flow around the hull and slip back into the channel astern. On the other hand, a simple wedge shape bow on a square flat bottom (toy boat shape) seemed to displace ice from the channel under the adjacent level ice.

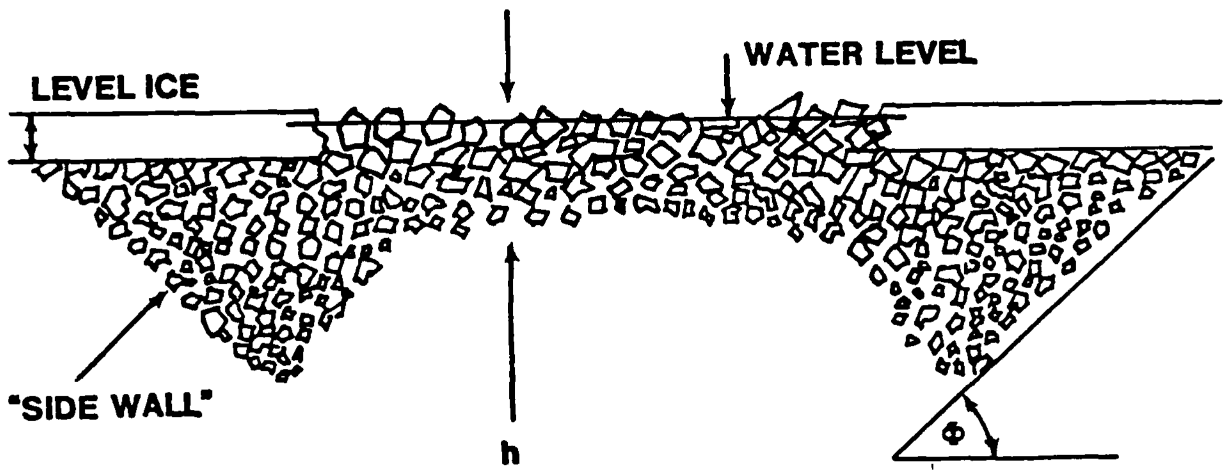

FIGURE 1. IDEALIZED CROSS-SECTION OF A BRASH-FILLED CHANNEL

Regardless of hull form, however, some broken ice is displaced under the adjacent level ice. This lateral displacement can be a small fraction of the broken ice remaining in the channel. Each additional passage through the channel displaces more ice under the level ice. This is an extremely subtle and rather insidious process since the submerged ice chunks form broad submerged walls on both sides of the channel. As these walls grow in depth, successive displacement of ice from the channel becomes more difficult. As more ice is formed in the channel through freezing and rebreaking, the side walls increase in depth and the broken ice in the channel also deepens. The side walls permit the pieces of ice in the channel center to stack. The lateral restraining force provided by the side walls balances the gravity force which tends to spread the ice pieces to a single layer. (In narrow shipping channels, of course, the side wall formation is not necessary. The bulkheads themselves supply the necessary barrier to spreading.) As the side walls build and the brash ice thickens in the center of the channel, the entire process is enhanced primarily by three factors. First, the side walls are strengthened by the freezing from above and the "cementing" together of the brash ice pieces by smaller pieces and frazil. Since the ice walls are undisturbed by rebreaking, they can solidify through freezing of the interstitial water. Second, the brash ice in the channel is cooled by the atmosphere to a temperature somewhere between the air and water temperatures. The situation of cold ice in water near its freezing point then exists and each time a brash piece is submerged, ice forms on its surface. Third, the exposure of open water patches and the agitation of the water during each ship passage enhance the heat loss through the surface of the channel relative to that through the adjacent level ice.

The combined effect of these factors results in a channel of rapidly increasing brash ice thickness surrounded by level ice which grows relatively slowly due to the insulating effect of the ice which impedes heat transfer from the water to the atmosphere. The accumulation of brash is, therefore, not dependent upon advection of rubble or the existence of a certain wind condition. It is the repeated passage of vessels in subfreezing conditions which is responsible for brash accumulation in most channels.

While ice is accumulating in the channel, each vessel passage agitates, rolls and grinds the individual pieces against one another and the ship's hull. Repeated passages result in well processed brash ice which is significantly modified in shape. We observed that the milling and grinding of the brash ice pieces appears to be independent of the action of the propellers. A very successful simulation of brash ice on 1/10 scale was accomplished in the tow tank entirely without the use of a propeller. The brash ice pieces are continually modified in shape but appear to rapidly approach a spherical form - very different from the original flat or tabular shape of the broken level ice pieces. This is not to say that "cannonball ice" consists of perfect spheres, but rather that the pieces are relatively spherical, their three dimensions being comparable. Eventually, an equilibrium distribution of sizes is approached. The range of these diameters may be from 10 cm to 3 m. The diameters of the largest pieces can exceed the level ice thickness due to accretion when the cold ice chunks are rolled about in the water. This accretion also aids in modifying the shape of the pieces towards a spherical form.

These observations of the formation of brash ice immediately lead us to an important modification of operational procedure. Once a channel is broken through level ice, continued patrolling of the channel (as is routinely done) is detrimental. The more passages made along the channel, the more brash ice forms and the more the submerged walls on the channel side deepen, permitting a thickening of the brash ice. If a brash-filled channel is left undisturbed, it will require far less effort to break a second time after some refreezing has taken place than it did initially if fewer degree days elapse between ice breaking runs than between the onset of the ice growth season and the initial ice breaking run. Certainly for ice breaking operations toward the end of the ice growth season, "maintaining" the channel by continually navigating it does only harm and, of course, consumes fuel needlessly. (This recommendation in presented in more detail in Section 5.0.)

To restate this recommendation: refreezing of the brash only slowly increases the brash ice strength. The best strategy after breaking a channel through level ice is to "leave well enough alone." Only under extremely severe environmental conditions persisting for long periods will it be more difficult to re-break the channel than it was to initially break it.

It should be mentioned that wind acting to close a brash-filled channel will exacerbate the navigation of the channel. As the channel is closed, lateral pressure on the brash increases and the depth of the brash ice must increase to balance the lateral force. Thus, lateral pressure and brash ice thickness are directly related through a hydrostatic type of relation.

4.0 BEHAVIOR OF THE BRASH ICE SUBSTANCE

The most puzzling and intriguing aspect of brash ice is its behavior which defies the intuition gained in level ice breaking and open water operations. Certain observations of an extremely simple nature can help to clarify the deformation of this substance under load (the rheology) in either a static or dynamic case. These observations are:

1. Brash ice which has not been refrozen has no tensile strength. It is merely a collection of ice chunks floating in water.
2. A brash-filled channel generally closes again when a vessel has passed through it.
3. Brash pieces roughly maintain their relative orientations after a vessel passage. That is, chunks at the center of the channel initially, are located close to the center of the channel after ship passage.

The appropriate rheological model for this behavior can, therefore, be neither elastic (as for level ice) nor that of a turbulent viscous fluid (as for open water). The lack of tensile strength precludes the first possibility while the lack of mixing of the ice pieces in the channel points to a non-turbulent flow. The proper description of the behavior of this material will be different from that of either level ice or open water.

With this very important caution in mind, we must search for a rheology which fits the behavior in a realistic range of strain rates or ship speeds. Some insight can be gained by observing brash ice in a loaded situation but at zero or very low strain rates, for instance the slow closure of a canal lock gate, the brash ice deforms and piles to a certain height for a certain stress. In fact, brash can be "piled up" to a certain maximum slope which corresponds to crushing failure. Another manifestation of this behavior is the formation of "noses" on the bows of blunt bowed lakers. Large "rafts" of brash ice are pushed ahead of the vessel as it progresses through the channel.

This type of behavior closely resembles that of a Mohr-Coulomb solid (a soil). Such materials are characterized by a cohesion, a shear strength and a friction angle or roughly the angle of repose. Their rheology can be summarized as:

$$\tau = C + \sigma \tan \emptyset \qquad (1)$$

where τ is the shear strength, C the cohesion, σ the normal stress on the substance and $\emptyset$ the friction angle.

Investigations into the strength of ice rubble have been performed with regard to stationary structures in slowly moving rubble fields. Evaluation of the variables of (1) has been performed by Keinonen and Nyman (1978) as well as others. Mellor (1979, 1980) has applied this rheology to ship resistance in thick brash ice. From our observations during 1980, we feel that Mellor's results are valid for slow ship speeds. That is, they predict when a ship can no longer make progress through a brash-filled channel. Before presenting his results, a few words of caution are necessary.

Mellor's development assumed a ship speed approaching zero; nowhere are the dynamics of the situation taken into account. As such, his results yield a force (roughly the integration over hull area of (1)). When this force exceeds the bollard pull of the vessel, the vessel can make no progress. Mellor's results, therefore, apply to only one point on a graph of resistance versus speed - zero velocity. We found that the resistance is constant over a range of low speeds but at a certain threshold increases with speed. This behavior is not predicted from Mellor's development but can be explained in terms of a strain-rate dependent rheology which is presented below following Mellor's work.

4.1 Brash Ice as a Mohr-Coulomb Solid

Mellor's (1980) paper is a very clear and illuminating piece of work. The summary of his findings is presented below for completeness.

Mellor begins by demonstrating that at very low ship speeds (on the verge of stalling) brash ice can be considered a Mohr-Coulomb solid. The failure criterion for such a substance is as stated in equation (1). Both the cohesion, C, and the friction angle, $\emptyset$, have been evaluated by several investigators with substantial scatter. However, the range of $\emptyset$ indicated by all the experimentation is between 42° and 58°. Mellor adopts 50° as a representative value.

The importance of this value is that dry granular solids generally have $\emptyset$'s less than 30°. The high $\emptyset$'s found for brash ice "suggest that inverted piles of brash could have very high angles of repose" meaning the formation of relatively steep-sided submerged walls is favored. The relatively large wall steepness permits rapid building of wall draft, since less material is required for steeper slopes.

With the cohesion ignored for a frequently navigated channel, Mellor develops expressions for the normal horizontal stress in terms of the vertical stress. The vertical stress is due to the weight of ice in air and in water, its porosity and the distance from the ice surface:

$$\sigma_z = (1-n)\rho_i g \left[t_1 - \left(\frac{\rho_w}{\rho_i} - 1\right)(z - t_1)\right] \tag{2}$$

where σ_z is the vertical component of normal stress, n is the porosity of thin ice, ρ_i is the density of ice, ρ_w is the density of the water, g is the acceleration of gravity, t_1 is the thickness of this ice layer below the waterline, z is the distance measured vertically downward from the ice surface. The horizontal stress can be expressed in terms of σ_z for two bracketing stress states - passive and active:

$$\text{(i) Passive, } \sigma_x = K_p\sigma_z = \left(\frac{1 + \sin\emptyset}{1 - \sin\emptyset}\right)\sigma_z \tag{3}$$

$$\text{(ii) Active, } \sigma_x = K_a\sigma_z = \left(\frac{1 - \sin\emptyset}{1 + \sin\emptyset}\right)\sigma_z \tag{4}$$

The passive state is encountered in deformed brash ice at its maximum compression before crushing failure and the active state at the maximum extension.

For a wide vertical plate "bulldozing" horizontally against a layer of cohesionless brash the resistance is composed of the contributions from above and below the water line. The maximum resistance encountered is just before crushing in the passive stress state. The total resistance per unit plate width is:

$$R = \frac{1}{2} \left(\frac{1 + \sin \phi}{1 - \sin \phi}\right) (1-n)\, \rho_i g \left(1 - \frac{\rho_i}{\rho_w}\right) t^2 \tag{5}$$

where t is the total thickness of the brash ice. If cohesion is included,

$$R = \frac{1}{2} \left(\frac{1 + \sin \phi}{1 - \sin \phi}\right) (1-n)\, \rho_i g \left(1 - \frac{\rho_i}{\rho_w}\right) t^2 + 2C \left(\frac{1 + \sin \phi}{1 - \sin \phi}\right)^{1/2} \tag{6}$$

the second term dominates only when C is large. Under such a condition, the resistance is essentially that of an intact ice sheet.

Representative values for the variables in (5) are

$\phi = 50^o$, $n = 0.36$, $\rho_i = 0.91$ g cm^{-3}, $g = 980$ cm s^{-2},
$\rho_w = 1.026$ g cm^{-3} (sea water) $\rho_w = 1.00$ g cm^{-3} (fresh water)

As the water density decreases, the resistance decreases. Such an effect can be achieved by bubbling air through the water. The experimental data on the efficacy of bubbler systems in brash ice are, however, inconclusive. At very low ship speeds, one would expect a strong influence on the resistance due to the bubblers. This is not observed (Vance 1980); rather, the most pronounced effect of the bubbler appears to occur at mid-speeds of about 9 knots.

Mellor also discusses the resistance in brash ice of a plate inclined at β^o to the vertical. He treats the submerged portion and expresses the resistance, R as a fraction of $R_{\beta=0}$ (where the plate is vertical). His results show that a plate inclined at 40^o to the vertical has 36% the resistance of a vertical plate. Most importantly, however, if the sloping plate extends well above and below the brash ice, the brash will simply pile up against the plate until resistance equal to that for a vertical plate is encountered. A ramp bow of a barge, for example will decrease the resistance only if the draft of the vessel is less than the height to which brash can pile. This height is predicted as less than about 6 times the initial brash thickness.

The resistance of a ship in brash ice is broken down into resistance of the bow section and resistance of the hull aft of the bow. The bow resistance is due to the bulldozing of the brash by normal thrust and tangential frictional forces. The dimensions of an idealized bow shape are shown in figure 2 (an adaptation of Mellor's figure 10). The resistance of the bow due to bulldozing is H_s.

$$H_s = 2(B/2 \sin\beta)\, R \sin\beta = BR, \tag{7}$$

where β is now a horizontal angle and R is given by equation (5).

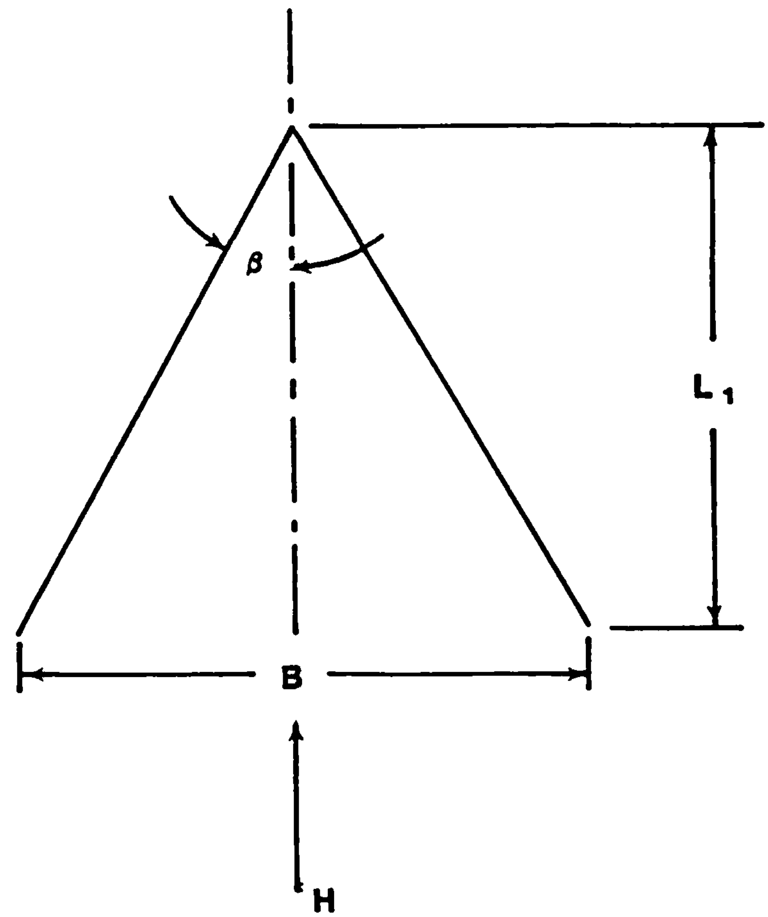

FIGURE 2. DIMENSIONS OF AN IDEALIZED BOW SHAPE

The frictional force component of the resistance of the bow is:

$$f = \mu_e R \tag{8}$$

where μ_e is the effective friction coefficient for the condition of pressure and water lubrication. The total resistance to motion of the wedge is:

$$H_f = (1 + \mu_e \cot\beta) BR \tag{9}$$

A very similar expression can be developed for a realistic bow shape as shown in figure 3. In this configuration,

$$H_f = 2\int_0^{B/2} R\,dy + 2\int_0^{L_1} \mu_e \quad R\,dx$$

$$= BR + 2\mu_e L_1 R$$

If the center line of the bow section is expressed as a multiple of the beam B,

$$L_1 = k_1 B,$$

where $2k_1 = \text{Cot}\,\beta$ '

and

$$H_f = (1 + 2k_1 \mu_e) BR \tag{10}$$

With very blunt bows or high friction coefficients interfacial slip between the hull and the brash ice becomes impossible and a "false nose" forms. The failure surfaces are then within the material itself. The "false nose" also known as an "ice prow" generally forms, with an angle of 90^o or slightly more at its apex.

The resistance of the hull aft of the bow is due to the ice-hull friction caused by the ice piled against the ships sides. The force per unit width on the sides, R', lies somewhere between R defined for the passive and active stress states. The afterbody friction can be expressed as:

$$F_{hf} = 2\mu_e L_2 R' \tag{11}$$

where L_2 is the length of the after-body section in continuous contact with the ice. If L_2 is expressed as a multiple (proportionality constant k_2) of the beam:

$$L_2 = k_2 B \tag{12}$$

then

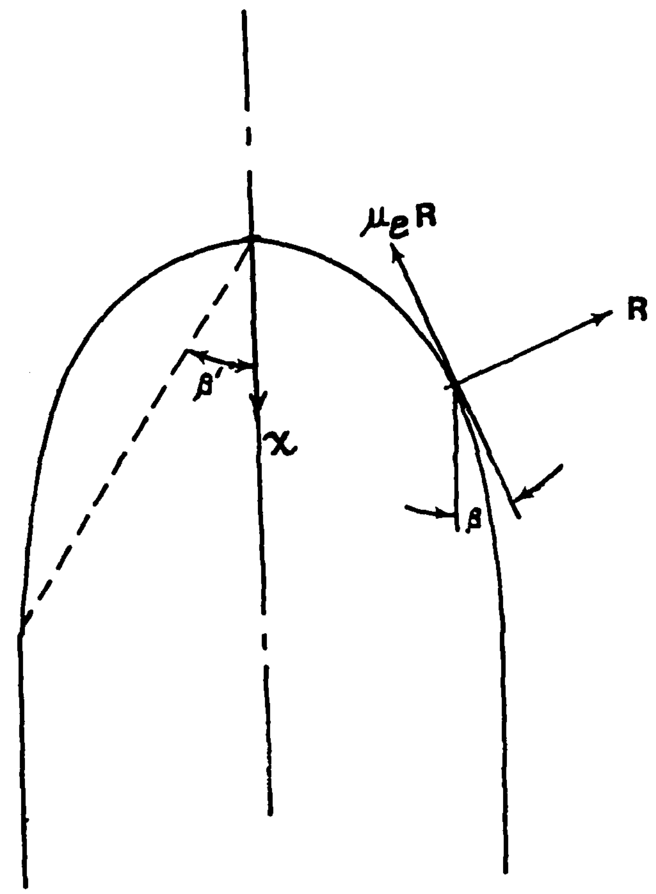

FIGURE 3. DIMENSIONS OF A REALISTIC BOW SHAPE

$$F_{hf} = 2\mu_e k_2 BR' \tag{13}$$
$$= 2\mu_e k_2 BNR \tag{14}$$

where N is a somewhat uncertain factor owing to the unknown stress state of ice. N is almost certainly, however, between 0.02 and 0.13, and Mellor estimates a likely value to be 0.1.

The total ship resistance can be written as the sum of the bow and after body resistance.

$$F_t = \left[1 + 2\mu_e(k_1 + k_2N)\right] BR \tag{15}$$
$$= A_2\ BR$$

which is merely an addition of (10) and (14). In (15), the numerical value of A_2 lies in the range of 1.3 to 2.6.

Mellor concludes his paper with an estimate of resistance based on conventional powering criteria for existing ships. He estimates that for a conventional Great Lakes carrier in fresh water brash ice, immobilization occurs at a ratio of brash ice thickness to beam, t/B of 0.094, so that a 30 m wide ship would be immobilized in 2.8 meters of brash ice.

The foregoing development is applicable for ships moving at vanishingly low speeds. It addresses the ultimate capability of a ship's performance in brash. The next question to be addressed is "how does resistance vary with ship speed?"

4.2 Experiments on Ship Resistance in Brash Ice

We approached this problem by first observing the deformation of brash ice during ship passage from existing films of vessels passing through brash ice which are on file at the U.S. Coast Guard R&D Center and at the U.S. Army Cold Regions Research and Engineering Lab (CRREL). From the films, the medium appeared to behave in a way that could be termed "viscous." That is, very little interchange of block position was observed (on the contrary, vigorous mixing is a characteristic of turbulent flow). The viscous supposition is supported if one considers the individual blocks as molecules. The relative size of the ship is perhaps 200 times the size of the "brash ice molecule." From this view, a very low Reynolds Number regime is indicated. The fluid-like behavior of the medium also suggests that the Mohr-Coulomb hypothesis applicable at very low strain rates might not apply at significant ship speeds. We felt that a transition might occur from soil-like to viscous behavior at a critical ship speed (or strain rate) where the brash ice medium was effectively fluidized.

4.2.1 Laboratory Tests

The hypothesis was examined in the laboratory at the U.S. Army Cold Regions Research and Engineering Laboratory, Ice Engineering Facility tow tank, as well as in the field. The first effort at CRREL was the creation of realistic brash ice in the laboratory. As far as we know, this was the first such attempt at reproducing brash in a tow tank rather than using preformed ice blocks. The procedure may be of interest to future investigators and is therefore described below in some detail.

The CRREL test tank (figure 4) is 120 feet long (36.5m), 30 feet wide (9.14m) and 8 feet deep (2.44m). The entire area can be lowered to a temperature of -10°F. A workable procedure for making brash ice in this laboratory was developed after several failures; the "recipe" is as follows:

1. The temperature of the fluid in the tow tank should be homogeneous and as near to the freezing point as practicable. In the CRREL tow tank, a roughly 2% urea solution in water was used to model the elastic properties of level ice. This solution could be classified as "brackish" in that complete thermal convection to the bottom of the tank did not occur upon surface cooling. To obtain a uniform temperature profile with depth, compressed air was fed in along perforated hose anchored to the tank's bottom. When the entire tank was within 0.1°C of its freezing point, further extraction of heat (without the bubbler operating) would rapidly form ice on the surface and the temperature gradients existing within the fluid would do little to retard the ice growth.

2. Initially, a level ice sheet of about 1 inch was grown and a 1/10 wooden scale model of a KATMAI BAY Class 140-foot (WTGB) ice breaking tug, ballasted with lead, was towed through the ice. A broken channel resulted with the characteristic size of ice pieces in the range of 1 to 2 feet. Perhaps 70 to 80% of the ice remained in the channel. In order to accumulate more ice in the channel, one could either wait for more ice to form in situ (with room temperature at +10°F) or in some way supply ice to the channel. Due to time constraints, we eventually opted for the latter choice.

3. A channel three beam widths wide was broken in the level ice. The ice sheets on either side of the channel were then freed from the tank walls and pushed toward the center of the channel simultaneously. This procedure introduced new level ice to the channel center while creating open water regions along the tank walls. The surface was allowed to refreeze until the ice was at least 1/2 inch thick along the walls.

4. The channel was re-broken, once again three beam widths wide, and re-closed by feeding ice into the tank center from the walls. This procedure was repeated until brash of the desired thickness was present in the channel.

5. A difficulty in this procedure is the continued growth of the initially formed level ice. After several breaking and re-closing procedures, the level ice thickness approached 6 inches. Converted to full scale this is equivalent to a thickness in the field

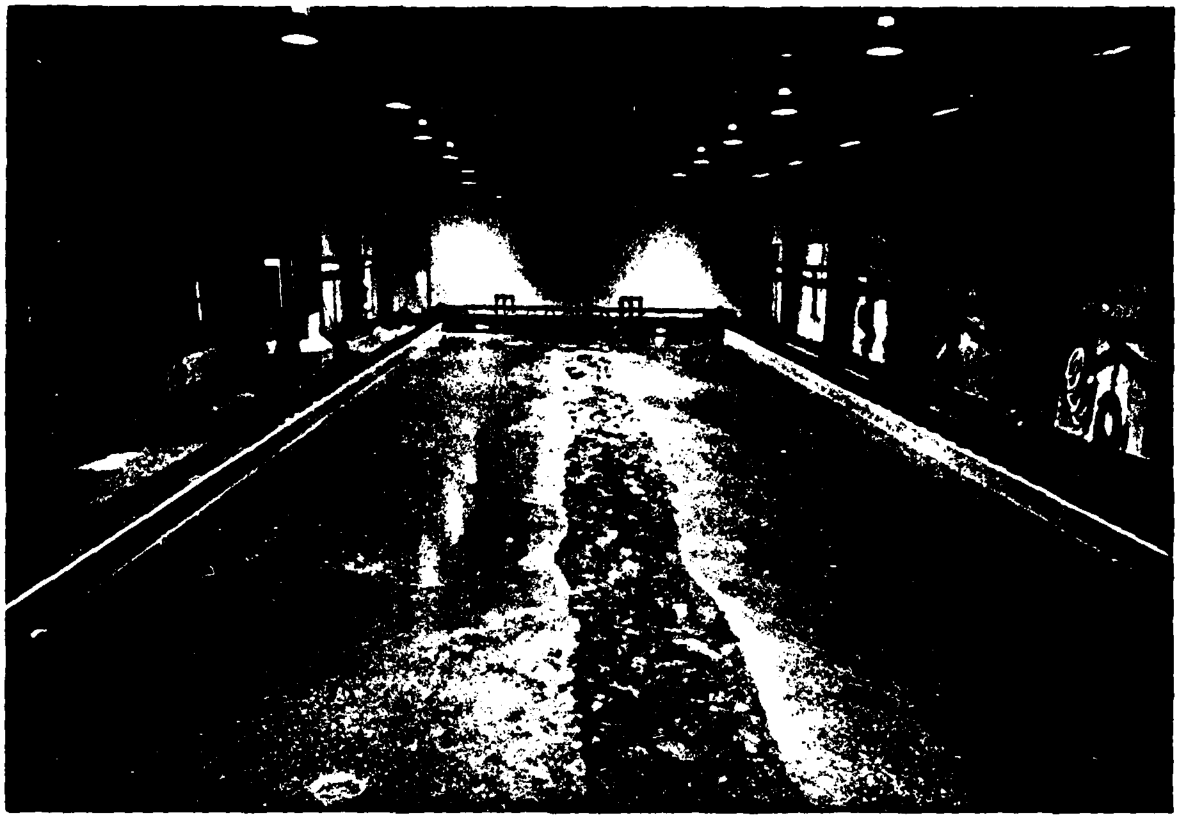

Figure 4. TOWING TANK AT CRREL ICE ENGINEERING FACILITY

of 5 feet - far more than the capability of a WTGB. As the ice grew at the channel sides, we were forced to resort to breaking pieces off with timbers wielded from the towing carriage. After 2 days of this procedure with the air temperature at $0^{o}F$, a very realistic brash-filled channel resulted with brash thickness about 2 to 4 inches, equivalent to 20 inches to 40 inches in full scale. Figure 5 shows the brash produced in the laboratory and that encountered in the field.

It is important to keep in mind that the above procedure artificially reproduces ice growth in the channel by supplying material from the flat ice sheet. The sheet must be pushed into the channel center after each run until the brash is the desired thickness.

After the brash was in place we performed, on the average, about 10 test runs per day where resistance force and velocity were measured. Over the course of these runs, very little brash ice growth was measured. This was due to the relatively short duration of the tests (about 1 week) and the continued lateral displacement of ice from the channel to the submerged rubble structure forming the channel walls. However, the brash pieces in the channel became progressively more rounded until after perhaps 20 passages an equilibrium distribution of sizes and shapes was reached. The pieces ranged from about 1/4 inch to 6 inches with about three fourths of the ice mass contained in pieces 1 to 10 inches in size.

The brash created behaved as if it were under lateral pressure. A "hole" made in the brash would spontaneously close. This behavior is due to the gravity and buoyancy forces acting on the brash. Towing the model through the brash caused no noticeable change in the appearance of the channel. This behavior implies that "pressure" (or lateral force due to wind stress) is important for ship resistance in brash ice only in that it increases the brash ice thickness. The depth of the brash is an accurate indication of lateral pressure and thus, pressure need not be considered independently from depth of the brash.

The towing tank experiments were designed to determine the variation of resistance with ship speed and "setup" of the brash since last disturbed. The second goal was unsuccessful due to limited time and the lack of precise control of air temperature. A curve of resistance versus speed with brash ice thickness as a parameter was established.

A 1:10 scale model of the KATMAI BAY Class icebreaking tug was towed through the prepared brash ice over the entire range of carriage speeds from 0.5 feet per second to 7 feet per second. Brash ice thickness varied from 3 to 6 inches. We were unable to randomize the brash thicknesses but the towing speed could be randomly selected so that the data would not be biased. Force was measured with a load cell installed in the model, which was connected with a universal joint to the towing post mounted on the carriage (see figure 6). The data from the model tests are shown in table 1. The model speed V, the measured resistance force, R, and the non-dimensionalized velocity and resistance, $\hat{V}$ and $\hat{R}$, are tabulated as well as a combination of non-dimensionalized variables which is explained below. The three data

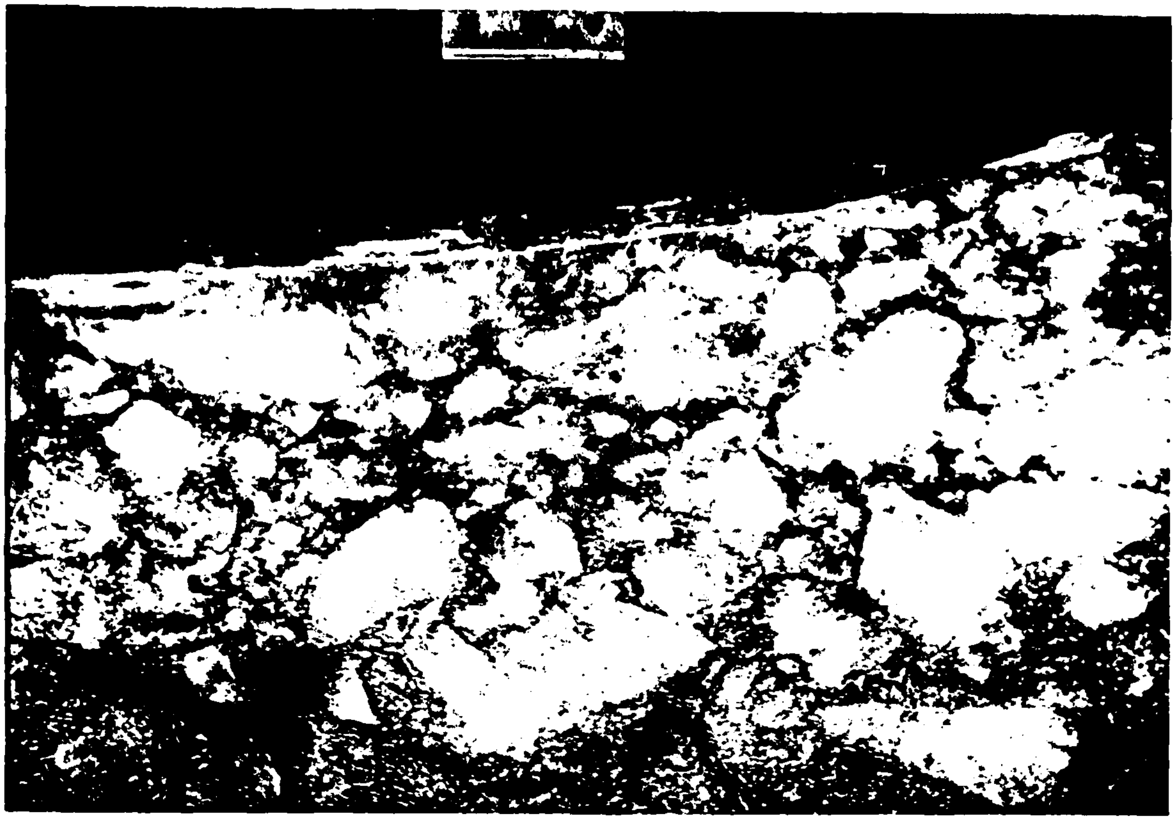

FIGURE 5a. Laboratory Brash Ice

FIGURE 5b. Natural Brash Ice

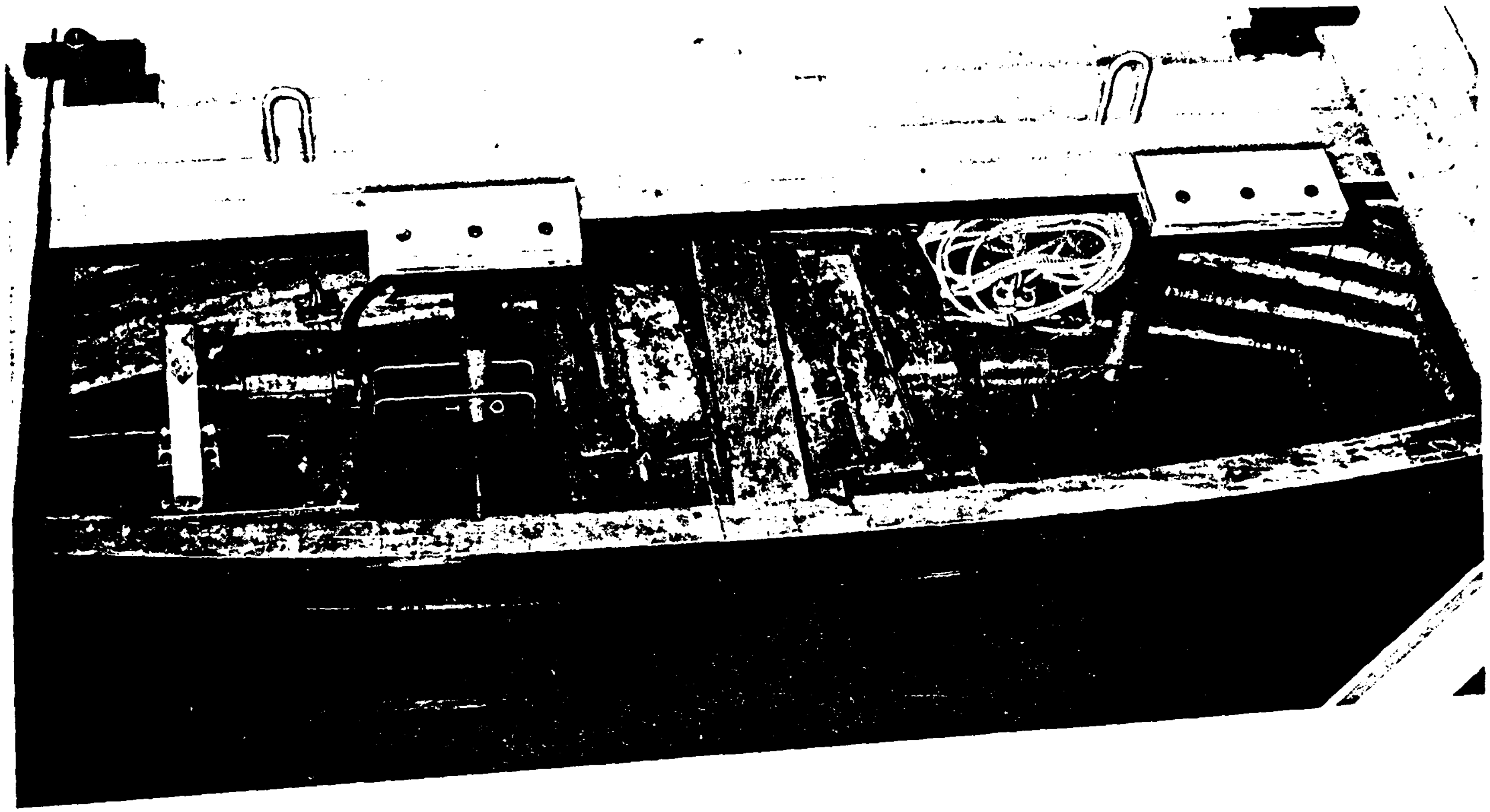

FIGURE 6. Scale model of KATMAI BAY showing towing post and force block forward (toward right) and yaw post and propeller motor aft (toward left).

TABLE 1

Model Test Data

R_o = 25 lbf L_o = 14.3f h_o = 3.5 in V_o = gL = 21.6 fps

V (fps)	R(lbf)	$\hat{V}$	$\hat{R}$	$\hat{R}/\hat{h}\hat{L}^{3/2}$	
1.0	22	.046	0.88	0.88	
1.2	25	.055	1.00	1.00	
2.0	25	.093	1.00	1.00	$\hat{h}$ = 1.00
3.0	27	.139	1.08	1.08	
4.0	33	.185	1.32	1.32	$\hat{L}$ = 1.00
5.0	41	.232	1.64	1.64	
6.0	40	.278	1.60	1.60	
7.0	55	.324	2.20	2.20	
0.66	35	.031	1.40	1.10	
1.0	38	.046	1.52	1.19	
1.5	30	.069	1.20	0.94	
2.0	38	.093	1.52	1.19	$\hat{h}$ = 1.28
2.2	40	.101	1.60	1.25	
3.2	40	.147	1.60	1.25	$\hat{L}$ = 1.00
4.2	55	.193	2.20	1.72	
4.6	60	.212	2.40	1.88	
5.0	57	.232	2.28	1.78	
5.7	65	.262	2.60	2.04	
6.5	55	.299	2.20	1.72	
0.5	70	.023	2.80	1.64	
2.0	74	.093	2.96	1.73	
4.0	88	.185	3.52	2.06	$\hat{h}$ = 1.71
6.0	114	.278	4.56	2.66	
7.0	140	.324	5.60	3.27	$\hat{L}$ = 1.00

$\hat{h}$ = h/ho $\hat{L}$ = L/Lo $\hat{R}$ = R/Ro $\hat{V}$ = V/Vo groupings apply to the three thicknesses of brash ice indicated. No information on the variation of resistance with scale can be obtained by experiments utilizing only one model size. Therefore, comparisons were made with field data collected by CRREL in 1979 (Vance 1980) and by the USCG R&D Center in 1980.

4.2.2 Field Tests

The field data were collected from the CGC KATMAI BAY in 1979 and the CGC BRISTOL BAY in 1980. In 1979, existing brash-filled channels were navigated in the St. Mary's River while thrust was measured at the instrumented thrust bearings. At the same time, ship speed was obtained with a Doppler radar and brash ice thickness measured directly by drilling and lowering a T-bar on a tape. An attempt at ascertaining the brash ice thickness with a helicopter-mounted impulse radar was made with rather inconclusive results. In 1980, the R&DC utilized the CGC BRISTOL BAY in the vicinity of Detroit. At this time, we did not completely instrument the ship. Rather, we relied upon the power and thrust data collected by Vance and recorded only the power to the propulsion motors, ship speed with Doppler radar and brash ice thickness. In 1980 we, too, made an attempt to measure brash ice thickness with impulse radar; however, we mounted the radar just ahead of the ship's bow on a fiberglass beam. While the radar appeared to function without noticeable interference from the vessel hull and accurately recorded level ice thickness, it proved to be unreliable in brash ice. First, the signal-to-noise ratio was extremely poor to the untrained eye. Second, the final thickness values supplied by experienced analysts at CRREL were in error by up to 100% (half the actual brash thickness was reported). We do, however, feel that the impulse radar can be developed into a valuable operational tool for the determination of level ice thicknesses.

In order to convert the thrust to resistance, a thrust deduction factor 0.2 was applied (Vance, 1980). The motor power was first converted to thrust by dividing by the velocity and that thrust reduced by 20% to yield resistance. The data from the full-scale tests are shown in table 2. Once again, the three data groupings correspond with data collected in three brash ice thicknesses. The last grouping was collected by computation of thrust from motor power and suffers from considerably more scatter than the first two groups.

The data from model and full-scale tests permitted an estimation of the effect of changing scale as well as changing brash thickness and velocity.

4.2.3 Interpretation of Data

We can make the general assumption that resistance, R, increases with brash thickness, h, with ship speed, V, and with ship length, L. The dependence on each of these variables is, however, unknown. One mathematical formulation for the foregoing statement is

TABLE 2

Field Test Data

R_o = 25 lbf $\quad L_o$ = 14.3f $\quad h_o$ = 3.5 in $\quad V_o$ = gL = 67.0

V (fps)	R($\text{lbf} \times 10^{-3}$)	$\hat{V}$	$\hat{R}$	$\hat{R}/\hat{h}\hat{L}^{3/2}$	
7.3	11.0	.109	440	1.24	
11.9	13.9	.178	556	1.57	
14.8	14.2	.221	568	1.60	
16.2	19.4	.242	776	2.19	$\hat{h}$ = 11.4
16.7	18.2	.249	728	2.04	
19.4	25.4	.290	1020	2.86	$\hat{L}$ = 9.8
21.2	25.0	.316	1000	2.82	
21.6	28.8	.322	1150	3.25	
22.0	27.8	.328	1110	3.14	
22.6	29.0	.338	1160	3.28	
0.89	10.1	.013	404	0.91	
4.0	8.1	.060	324	0.74	
4.5	8.8	.067	352	0.80	
8.4	14.3	.125	573	1.30	$\hat{h}$ = 14.3
12.1	16.4	.181	656	1.49	
12.8	16.6	.191	664	1.51	$\hat{L}$ = 9.8
18.2	25.9	.272	1040	2.36	
19.4	26.3	.290	1050	2.39	
20.4	30.9	.304	1240	2.81	
26.2	30.4	.392	1220	2.76	
4.0	13.4	.060	536	1.06	
8.5	11.1	.127	440	0.85	
11.1	20.5	.166	820	1.57	$\hat{h}$ = 17.0
11.8	32.8	.176	1310	2.52	
13.8	24.1	.206	964	1.84	$\hat{L}$ = 9.8
14.2	23.4	.212	936	1.79	
16.4	47.7	.245	1910	3.66	
17.0	45.5	.254	1820	3.49	

$\hat{h}$ = h/ho $\qquad \hat{L}$ = L/Lo $\qquad \hat{R}$ = R/Ro $\qquad \hat{V}$ = V/Vo

$$\hat{R} = K\ \hat{h}^m\ \hat{L}^n\ \hat{V}^p \tag{16}$$

where K is a nondimensional constant, m, n and p are undetermined exponents and the circumflexes over the variables denote that they each have been nondimensionalized. That is,

$$\hat{h} = h/h_0, \quad \hat{L} = L/L_0, \quad \hat{V} = V/V_0, \quad \hat{R} = R/R_0 \tag{17}$$

where the subscript zero denotes a reference value.

In our experiments, we measured each of the four variables and sought to express R in terms of the other three. This was accomplished by first using the ship length and gravity, g, to nondimensionalize velocity:

$$\hat{V} = V/\sqrt{gL} \qquad \text{i.e., } V_0 = \sqrt{gL} \tag{18}$$

This non-dimensionalization implies a scaling consistent with Froude similitude as applied for ship resistance in open water. Due to our initial ignorance of the brash ice medium, we had no prior justificaion for this scaling, other than to be consistent with other ship resistance work.

The non-dimensionalized resistance combined with h and L was then plotted versus $\hat{V}$: That is, $\frac{\hat{R}}{\hat{h}^m\ \hat{L}^n}$ was plotted versus $\hat{V}$. The data indicated that the resistance was proportional to the brash ice thickness raised to a power of about 1. In addition, we expected the resistance to be roughly proportional to the area of hull in contact with the brash, but at most to a cube of a linear dimension. Plots were constructed for m = 1, 3/2, 2 with n = 1, 3/2, 3/4, 2. Most combinations were clearly inappropriate by comparing just a few full-scale and model-scale experiments. The best fit was obtained with m = 1, and n = 3/2 (see figure 7). The fit of both the laboratory and full-scale data to this curve is good. Four of the outlying points are due to our coarse estimates of thrust from motor power. Nevertheless, these points, also bracket the curve

$$\frac{\hat{R}}{\hat{h}\ \hat{L}^{3/2}} = K\ \hat{V}^{3/2}\ . \tag{19}$$

However, in none of the attempted fits could the data be matched at low speeds to the 3/2 order parabola. In each data set, there is a critical speed, $\hat{V}_c$, below which the resistance remains constant. For the 140-foot hull, $\hat{V}_c$ = 0.12.

The constancy of resistance over the $\hat{V}$ range 0 to 0.12 is striking and consistent with the Mohr-Coulomb behavior of brash ice developed by Mellor. We conclude, therefore, that brash ice has a rheology dependent upon strain rate (or ship speed). At low speeds, it behaves as a Mohr-Coulomb solid. Above a certain critical speed, the resistance is very much velocity dependent and brash behaves as a viscous fluid, in fact, a fluid in LAMINAR FLOW.

The last statement is based on the results of investigations of laminar flow over flat plates (Schlichting, 1979). Schlichting shows that for a flat plate wetted on both sides in laminar flow, the drag, D can be written,

$$D = 1.33\ b\ V^{3/2} \ell^{\ 1/2} \quad (\rho\mu)^{1/2} \tag{20}$$

where b is the height of a vertical plate in horizontal flow parallel to its length, V is the velocity of the flow, ℓ the length of the plate, ρ the density of the fluid and μ the dynamic viscosity.

For a given substance

$$D = K\ bV^{3/2} \ell^{\ 1/2} \tag{21}$$

This expression shows the same velocity dependence as (19) and reinforces our conception of a laminar flow of brash around the ship. On the other hand, the drag on the plate is proportional to its length to the one half power while the drag on a vessel in brash shows a three quarters power dependence on its length. That is,

$$\text{ship in brash} \qquad R \sim \hat{V}^{3/2}\ \hat{h}\hat{L}^{3/2} \sim V^{3/2}\ hL^{3/4} \tag{22}$$

$$\text{flat plate laminar flow} \qquad R \sim V^{3/2}\ b\ell^{1/2} \tag{23}$$

This slight discrepancy might be explained through experimental uncertainties or in terms of the difference between the geometry of a ship hull and a flat plate. While the brash thickness, h, is probably a good analog to the height of the plate along the side of the ship, the analogy breaks down in the vicinity of the bow. In this region, the hull area in contact with the brash is proportional to L^2 rather than to L as it is along the ship's sides since the bow contact area is not vertical. In other words, the linear increase in ship length enhances the area of the bow as the square of the length.

The dependence of drag on the square root of the length in the direction of flow remains the same. By maintaining a constant brash thickness but increasing the ship length, we enhance the drag by increasing the length the brash travels along the ship <u>and also</u> by increasing the surface area. We might more properly write (22) as

$$\text{ship in brash:} \qquad R \sim V^{3/2}\ h\ell^{\ 1/2}\ L^{1/4} \tag{24}$$

where lower case "ℓ" expresses the dependence on length of flow regime and upper case "L" is hull length. The last factor reflects the increase in bow area.

The strain rate dependent rheology can be mathematically expressed as

$$\frac{\hat{R}}{\hat{h}\ \hat{L}^{3/2}} = C_1 \qquad \hat{V} < \hat{V}_c \tag{25a}$$

$$\frac{\hat{R}}{\hat{h}\ \hat{L}^{3/2}} = C_1 + C_2\ (\hat{V}-\hat{V}_c)^{3/2} \qquad \hat{V} > \hat{V}_c \tag{25b}$$

C_1, C_2 and V_c can be directly determined from the plot of the nondimensionalized data. The constants arising from the arbitrary nondimensionalization of R, h and L (where R_o = 25 lbf, L_o = 14f and h_o = 0.3f) were C_1 = 1.0 and C_2 = 23.4. The nondimensionalization of velocity by the $\sqrt{gh}$ is somewhat less arbitrary and $\hat{V}_c$ = 0.12

The resulting two regime curve is plotted in figure 7 where it is superimposed on the data. The horizontal portion of the curve at speeds less than $\hat{V}_c$ = 0.12 is the regime over which the material acts as a Mohr-Coulomb solid. At $\hat{V} = \hat{V}_c$ the behavior of the medium changes. We have no evidence that this transition is discrete as is, for example, the transition from sub-critical to super-critical channel flow.

The fluidization of the brash which occurs at $\hat{V}_c$ is probably due to dynamic fluid forces acting on the individual brash pieces; a situation similar to the behavior of beach sand subjected to an energetic wave field. A familiar example of fluidization is the process by which a small pile of insoluble substance (such as sand) in a beaker of water is suspended by stirring.

At some ship speed ($\hat{V}_c$) the turbulent kinetic energy of the flow of water around the hull overcomes the gravitational potential energy associated with the stacking of the floating brash pieces. At this point, the individual brash pieces are supported more by dynamic fluid forces than hydrostatic or gravity forces: the brash is suspended in a regime of turbulent water flow even though the large scale motion of the ship through the brash is laminar flow!

5.0 RECOMMENDATIONS

In this study, the behavior of the material called "brash ice" was investigated, and a simple rheology developed. It is somewhat beyond the range of expertise of the present author to apply these physical characteristics to the operating of vessels. However, I have hazarded a few tentative recommendations below:

1. A practical outcome of this investigation is the knowledge that brash ice resistance is constant with speed up to a critical value. In terms of operation, therefore, ships in brash should operate at the critical velocity, $\hat{V}_c$, in order to consume the least fuel while negotiating the track line in the shortest time.

The time of transit, TT, is equal to the length of the channel divided by the velocity:

$$TT = x/v \tag{26}$$

The power output, P, is a function of the resistance and speed

$$P = v\, R_{(v)}\ . \tag{27}$$

If the specific fuel consumption is y which is expressed in units of pounds of fuel per horsepower per hour, then the total fuel consumption FC is

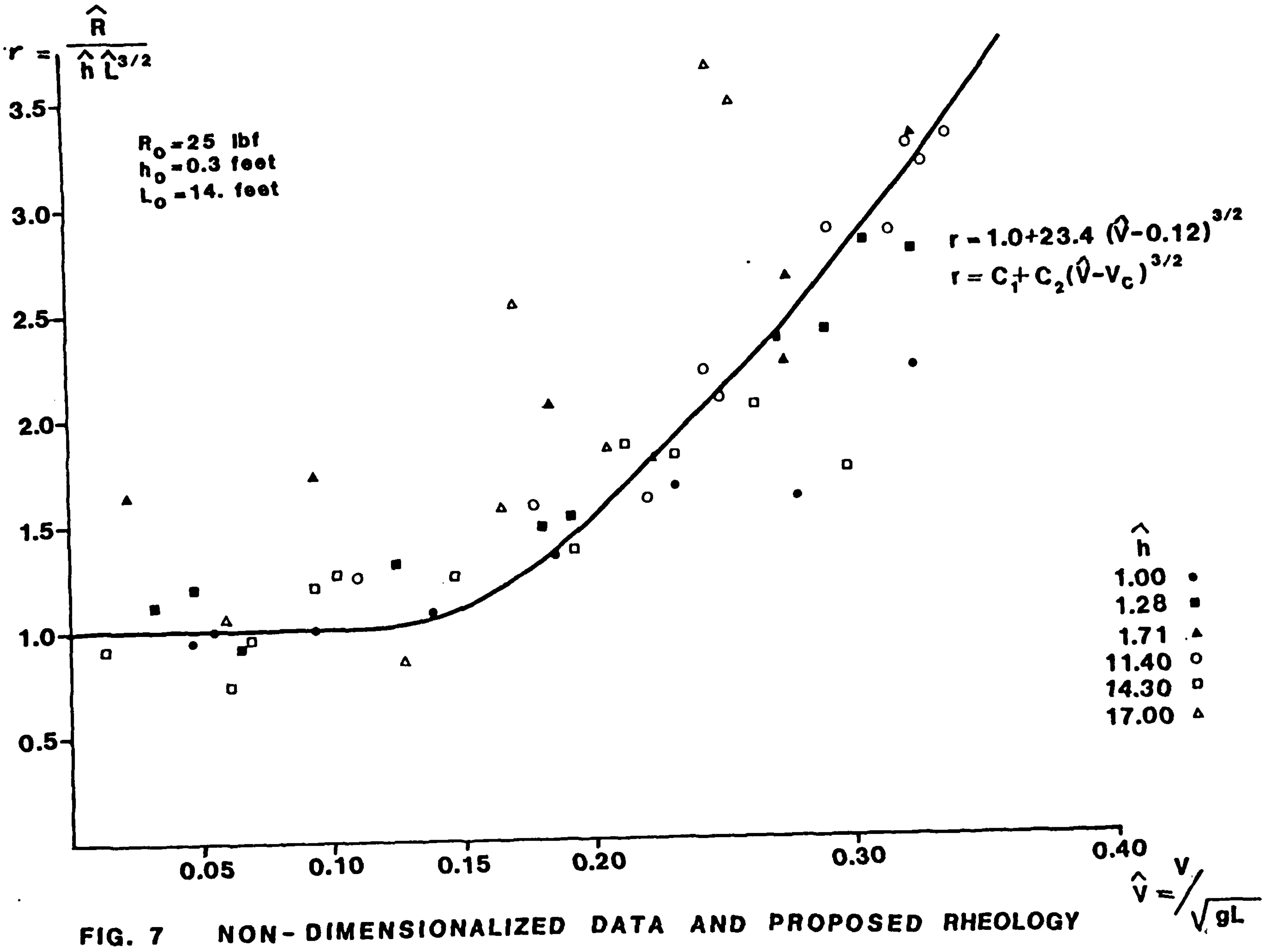

FIG. 7 NON-DIMENSIONALIZED DATA AND PROPOSED RHEOLOGY

$$FC = y\,P\,TT = yvR_{(v)}x/v = y\,R_{(v)}x \qquad (28)$$

In the above, R is a function of velocity but y, the specific fuel consumption, and x the trackline length are constant. Therefore, the same amount of fuel is consumed for a given trackline length for that regime where the resistance is constant with velocity. The same amount of fuel is consumed over a given distance in brash at any speed less than the critical $\hat{V}_c$. Optimum operational procedure would, therefore, be to run at the critical speed in order to minimize time of transit. V_c can be determined for all classes of icebreakers.

2. As stated earlier, level ice, when first broken, forms a channel filled (usually incompletely) with brash-rubble. This substance will refreeze at a rate dependent upon the air temperature. Unless the temperature is very extreme and the time between passages long, the channel need not be routinely re-broken (or patrolled). Such patrolling will serve only to increase the growth rate of the brash. A guide to the proper action follows.

Ice thickness is proportional to the square root of the accumulated degree-days where a degree-day (DD) is the time integral of temperature deviation below the freezing point:

$$DD = \int_0^T \theta\, dt \qquad (29)$$

where θ is the air temperature below the freezing point of water (fresh or salt), t is time and T is the period in days over which freezing occurs. Level ice thickness h_L, is therefore

$$h_L = \alpha\sqrt{DD}. \qquad (30)$$

where α is an empirical constant which must be evaluated for varying conditions. The square-root dependence is due to slower ice growth as the ice thickness is increased caused by the insulating effect of the ice.

When the channel is first broken, the brash has no cohesion and will, of course, be considerably easier to transit than the unbroken level ice. The brash resistance only approaches that of the parent level ice sheet when it is entirely "frozen in"; that is when all the spaces between the brash pieces are refrozen. This can only occur when the elapsed degree-days are comparable to the accumulated degree days since the beginning of the freezing season. "Comparable" is an important qualification. The brash-filled channel will freeze more quickly than open water. We can only guess what fraction of the accumulated degree-days is required to render the channel as difficult as the parent ice sheet. A reasonable assumption is that this fraction is ~ 0.3

An example with numerical values may be of help in clarifying this matter. Say a level sheet of fresh water ice 2 feet thick has formed. The number of degree-days required to form an ice sheet of this thickness can be computed from (30), where the value of α may be taken as 0.6 inch/(^{o}F-day)$^{1/2}$

The value of α, varies with snow cover, wind speed, salinity and heat flux. The value mentioned here was computed for the very low salinity (1 $^o/_{oo}$) northern Gulf of Bothnia.

(Sandkvist, 1980). Using Sandkvist's value for α, the number of elapsed degree-days can be computed

$$DD = \left(\frac{h_L}{\alpha}\right)^2 = \left[\frac{24 \text{ in}}{0.6 \text{ in}/(^{o}\text{F day})^{1/2}}\right]^2 = 1600 \qquad (31)$$

1600 degree days were responsible for the growth of the level ice. If we assume that 0.3 of this cooling will freeze the brash-filled channel to 24 inches depth, then 480 degree days would have to elapse before the cohesive forces between the brash blocks render the channel as difficult to navigate as the parent ice sheet. Four hundred eighty degree days would elapse at a temperature of -16°F constant over a period of 10 days.

This computation is of course a rough indicator only, but it would be extremely unlikely that the channel would require re-breaking more often than every 5 days under these conditions.

3. Frequent repeated passages of brash-filled channels enhance the growth rate of ice in the channel. Therefore, passages should be minimized.

The chief factor contributing to enchancement of ice growth in repeatedly navigated channels is the re-exposure of open water to the atmosphere. This process has been investigated by Sandkvist (1980) who found the growth rate of brash thickness, H_E, could be mathematically expressed as

$$H_E = H_S + \sum_i H_i, \qquad (32)$$

where H_S is the level ice thickness before the first passage and H_i are the incremental ice thicknesses added between passages.

Sandkvist expressed H_i in the form of (30), but he found the value of the brash ice proportionality constant, α_B, to be about 0.3 inches/ $(^{o}\text{F-day})^{1/2}$, i.e.

$$H_i = \alpha_B \sqrt{(\Delta DD)_i} \qquad (33)$$

where $(\Delta DD)_i$ is the number of degree days between passage i-1 and passage i. Although α_B is smaller than α, Sandkvist still found more rapid ice growth in the channel. This is due to the square root dependence on degree days. The growth curve is parabolic and frequent rebreaking keeps the growth rate high since the effective thickness is near zero where the highest growth rate occurs.

Sandkvist found at temperatures around 0°F that the level ice thickness reached about 3 feet in early April. The brash ice thickness in a channel navigated 33 times between December and April (upon which (33) is based) was 8 feet.

6.0 SUMMARY

We have presented here Mellor's theory of the ultimate resistance to a vessel in brash ice, and our empirical formulation of the variation of resistance with vessel speed and the optimum speed of operation. In addition, a dual character of brash ice is presented in which a transition between Mohr-Coulomb and viscous behavior is observed.

The formation of the substance is described as well as means to simulate it in the laboratory. The success of our laboratory effort implies that routine testing in brash ice could be easily implemented to determine V_c for all classes of vessels operating in brash ice.

The important role of frequent passages through brash-filled channels in the accretion of the substance is emphasized.

REFERENCES

Keinonen, A. and T. Nyman (1978). An Experimental Model Scale Study on the Compressible, Frictional and Cohesive Behavior of Broken Ice Mass, Int. Assoc. of Hyd. Res. Symposium, Lulea, Sweden, pp 335-353.

Levine, G.H., R.P. Voelker, and P.B. Mentz (1974). Advances in the Development of Commercial Ice-Transiting Ships. Society of Naval Architects and Marine Engineers, Annual Meeting Nov. 1974, 26 pps.

Mellor, M. (1979). Towing Ships through Ice Clogged Channels by Warping and Kedging. CRREL Report 79-21 (prepared for U.S. Coast Guard), 21 pps.

Mellor, M. (1980). Ship Resistance in Thick Brash Ice. Cold Regions Science and Technology V. 3, pp. 305-321.

Sandkvist, J. (1979). Accelerated Growth of Ice in Ships' Tracks caused by Repeated Passages - observation results. University of Lulea Division of Water Resources Engineering Internal Report 1979: 07, 63 pps.

Schlichting, H. (1979). Boundary Layer Theory. McGraw-Hill, New York. 817 pps.

Vance, G. (1980). Analysis of the Performance of a 140-foot Great Lakes Icebreaker: USCGC KATMAI BAY. CRREL Report 80-8. 28 pps.

ADDITIONAL BIBLIOGRAPHY

Cheng, S. T. and J.C. Tatinclaux (1977). Compressive and Shear Strengths of Fragmented Ice Covers - A Laboratory Study. Iowa Institute of Hydraulic Research Report #206. NTIS # AD A045246, 82 pps.

Milano, V.R. (1975) Ship Resistance to Continuous Motion in Mush Ice. Soc. Nav. Arch. & Mar. Engrs. Ice Tech Symposium, Montreal, Apr. 1975, 32 pps.

Sneck, H.J. and J.M. Kaufman (1976). Low Friction Hull Coating for Icebreakers: Analysis of Ice Breaking in Particulate Ice, Phase II, Part III. USCG Report No. CG-D-33-76. NTIS # AD-A024 898, 43 pps.

Welsh, J.P. and B.T. Kingsbury (1974). Characterization of Slush Ice in the Great Lakes. Coast Guard Report # CG-D-45-75. 17 pps.

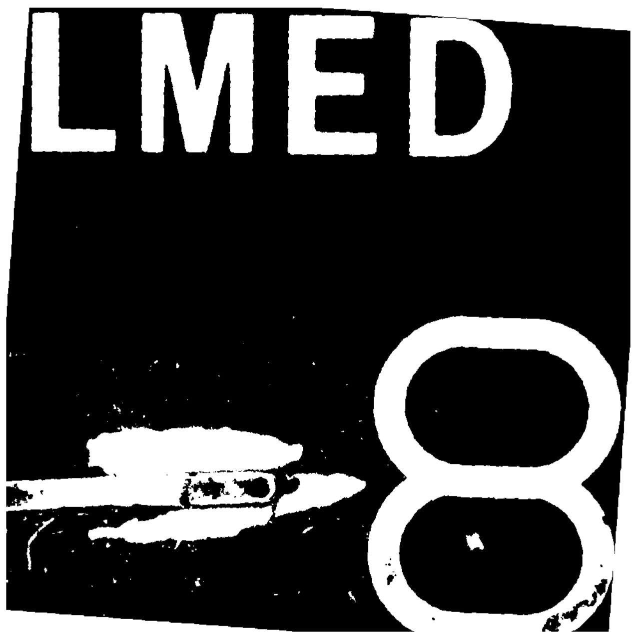
LMED
8